

## PhotoD: LSST photometric distances out to 100 kpc.

GREG J. SCHWARZ <sup>1</sup>, AUGUST MUENCH,<sup>1</sup>

(AAS JOURNALS DATA EDITORS)

BUTLER BURTON,<sup>2,3</sup> AMY HENDRICKSON,<sup>4,\*</sup> JULIE STEFFEN,<sup>5,1</sup> MAGARET DONNELLY,<sup>6</sup>

<sup>1</sup>*American Astronomical Society*

*1667 K Street NW, Suite 800*

*Washington, DC 20006, USA*

<sup>2</sup>*Leiden University*

<sup>3</sup>*AAS Journals Associate Editor-in-Chief*

<sup>4</sup>*TeXnology Inc.*

<sup>5</sup>*AAS Director of Publishing*

<sup>6</sup>*IOP Publishing, Washington, DC 20005*

### ABSTRACT

This example manuscript is intended to serve as a tutorial and template for authors to use when writing their own AAS Journal articles. The manuscript includes a history of AAST<sub>E</sub>X and documents the new features in the previous versions as well as the bug fixes in version 6.31. This manuscript includes many figure and table examples to illustrate these new features. Information on features not explicitly mentioned in the article can be viewed in the manuscript comments or more extensive online documentation. Authors are welcome replace the text, tables, figures, and bibliography with their own and submit the resulting manuscript to the AAS Journals peer review system. The first lesson in the tutorial is to remind authors that the AAS Journals, the Astrophysical Journal (ApJ), the Astrophysical Journal Letters (ApJL), the Astronomical Journal (AJ), and the Planetary Science Journal (PSJ) all have a 250 word limit for the abstract<sup>a)</sup>. If you exceed this length the Editorial office will ask you to shorten it. This abstract has 182 words.

**Keywords:** Distance measure (395) — Interstellar extinction (841) — Photometry (1234) — Stellar distance (1595) — Two-color diagrams (1724)

### 1. INTRODUCTION

Thanks to the *Vera C. Rubin* observatory's *Legacy Survey of Space and Time* (LSST), for the first time in history, an astronomical catalog will contain more Milky Way stars than there are living people on Earth – of the order 10-20 billion, depending on model assumptions. In order to map the Milky Way in three dimensions, distances to these stars must be accurately estimated. In this paper we describe a method that will deliver

LSST-based stellar distance estimations complementary to *Gaia*'s state-of-the-art trigonometric parallaxes and reach about 10 times further, to approximately 100 kpc. These results will be transformative for the studies of the Milky Way in general, and the stellar and the dark matter halo in particular as never before was there a survey that simultaneously observed roughly two thirds of the sky, to the co-added depth of  $r \approx 26$  mag.

**A bit about the importance of the distance estimation in the MW, dust implications (for extragalactic science too).**

There are a variety of astronomical methods to estimate distances to stars, ranging from direct geometric (trigonometric) methods for nearby stars to indirect methods based on astrophysics for more distant stars.

Corresponding author: August Muench

[greg.schwarz@aas.org](mailto:greg.schwarz@aas.org), [gus.muench@aas.org](mailto:gus.muench@aas.org)

<sup>a)</sup> Abstracts for Research Notes of the American Astronomical Society (RNAAS) are limited to 150 words

\* AASTeX v6+ programmer

51 Mention Bailer-Jones et al. (2021), Gordon et al.  
 52 (2016), Green et al. (2014, 2015, 2019), Jurić et al.  
 53 (2008) and Lallement et al. (2014), Queiroz et al. (2018).  
 54 Layout of the paper is...

## 55 2. METHOD

56 The photometric distance estimation method (here-  
 57 after **photoD**) is conceptually quite simple and relies on  
 58 the strong correlations between the stellar colors and  
 59 spectral energy distributions (SED) for dominant stel-  
 60 lar populations. The stellar spectral energy distribu-  
 61 tions, and consequently colors, are determined by the  
 62 effective temperature ( $T_{\text{eff}}$ ), the surface gravity ( $g$ ), and  
 63 the metallicity ( $[M/H]$ ), or alternatively, by the absolute  
 64 magnitude in band  $b$  ( $M_b$ ),  $[M/H]$  and age.

65 The distributions that describe these correlations are  
 66 obtained either from models or from observations. For  
 67 example, the distribution of stellar SEDs in the color-  
 68 color diagram in Figure 1 provides key insights in stel-  
 69 lar evolution and classification of different stellar popu-  
 70 lations such as main-sequence stars, giant stars, white  
 71 dwarf stars, a majority of unresolved binary stars and  
 72 even extragalactic objects. Analogous distributions  
 73 are responsible for the abundant structure seen in the  
 74 Hertzsprung-Russell diagram (HRD).

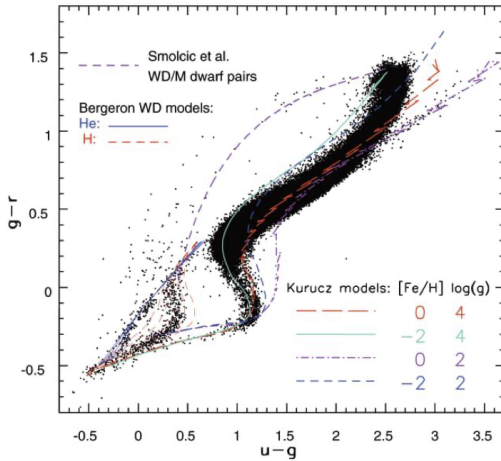


FIG. 23.—The  $g-r$  vs.  $u-g$  color-color diagrams for all nonvariable point sources constructed with the improved averaged photometry (dots). Various stellar models (Kurucz 1979; Bergeron et al. 1995; Smolčić et al. 2004) are shown by lines, as indicated in the figure.

**Figure 1.** Color-color diagram. Add a version with overlaid evolutionary tracks in order to emphasize the required precision of the photometry required to disentangle the dwarfs and giants and different metallicities. Are ev. tracks with different metallicities overlapping? Can there be a situation where there is confusion between giants and dwarfs with different metallicities?

75 Metallicity is an important factor in these correla-  
 76 tions, as it has a strong effect on the luminosity of the

77 stars. This is reflected in the width of the main stel-  
 78 lar loci of the color-magnitude diagrams (CMD) of the  
 79 stellar populations observed at the same distance and  
 80 the two-color diagrams (quantify), as seen in Figure 2.  
 81 The best photometric estimators of metallicity are col-  
 82 ors whose shorter-wavelength component includes the  
 83 metal absorption bands at near-UV wavelengths, short  
 84 of Balmer break ( $300 \lesssim \lambda \text{ [nm]} \lesssim 400$ ). Therefore,  
 85 the LSST has a comparative advantage over the sur-  
 86 veys lacking  $u$ -band measurements, and could provide  
 87 accurate distances within the range of 5-10%. A plot  
 88 of model spectra, fixed,  $\log(g)$  and  $T_{\text{eff}}$ , several different  
 89 metallicities?

THE ASTROPHYSICAL JOURNAL, 783:114 (16pp), 2014 March 10

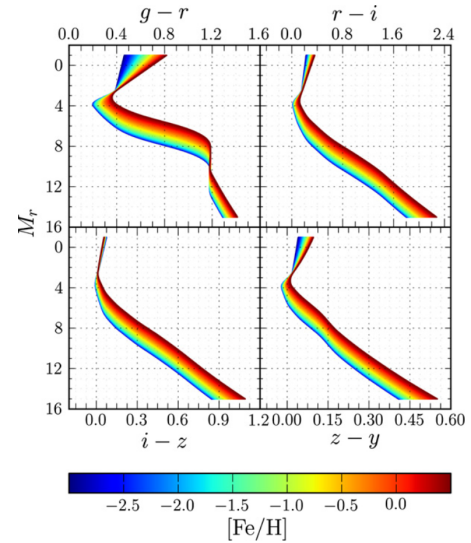


**Figure 1.** Model stellar colors as a function of absolute  $r$  magnitude and metallicity in Pan-STARRS 1 passbands. The stellar templates are based on PS1 color-color relations, and color is related to absolute magnitude and metallicity by SDSS observations of globular clusters (Ivezić et al. 2008a). Our empirical templates therefore assume an old stellar population. While the main sequence below the turnoff is nearly invariant with age, the giant branch and the location of the turnoff do, in reality, vary considerably with age. For this reason, we expect our inferences for main-sequence stars to be more accurate than those for giants. The narrowness of the kink at  $M_r \simeq 2.4$  is an artifact of our models (see Section 4.1).

**Figure 2.** Yadayada.

90 Extinction is a major source of systematic errors in the  
 91 process of luminosity and distance determination. The  
 92 fact that the extinction vector is nearly parallel to the  
 93 main stellar locus in the two-color diagrams gives rise  
 94 to degeneracies that complicate the determination of the  
 95 stellar type. An example is displayed in Fig. 3, where in  
 96 the left panel any of the different star types designated  
 97 as 1,2 and 3 can have the same observed colors as the  
 98 star marked as "Obs". This degeneracy is a result of the  
 99 combination of colors chosen for the two-color diagram  
 100 and depends on the adopted extinction curve  $R_V$  and  
 101 the position on the stellar locus. The degeneracy can be

broken if several different colors are used, particularly those towards the infrared, where the stellar locus is not kinked and the extinction vector is not parallel to it (as shown in the right panel of the Figure 3).

Explain the choice of  $R_V$ .

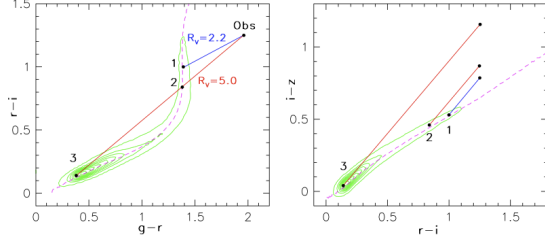


Figure 3. Extinction & degeneracies.

$$\begin{aligned}
 L &= 4\pi\sigma R^2 T^4 \\
 g &= \frac{GM}{R^2} \\
 L &= 4\pi\sigma \frac{GM}{g} T^4 \\
 \mu &= m_b - M_b (-A_b) \\
 \log(d) &= 1 + \frac{\mu}{5}
 \end{aligned}$$

Another important degeneracy arises from the fact that even for a fixed  $T_{eff}$  and  $[M/H]$ , the  $\log(g)$  thus luminosity are not uniquely determined. A way to mitigate this issue is to adopt a Bayesian framework

overlap in the color-color diagrams (e.g. Figure 1).

This effectively means that for a fixed  $T_{eff}$  proxy ( $g-r$ ),

Given the observed colors, and assuming small errors, the estimation of stellar parameters is relatively straightforward and follows one of the two possible approaches: empirical or model-based. In the former case, the case the underlying distribution to which the observations are matched is obtained from (ideally) spectroscopic and photometric observations, while in the latter case the distributions are generated from population synthesis models.

Advantages & disadvantages of the model-based and empirical approaches, how model based approaches can be improved by adding empirical information for specific cases.

Gordon et al. (2016) na BEAST webu imaju zgodne diagrame; možda bi i mi mogli nešto tog tipa napraviti, bar za draft, primjer

### 3. TESTING

### 4. DISCUSSION

## APPENDIX

## REFERENCES

- Bailer-Jones, C. A. L., Rybizki, J., Fouesneau, M., Demleitner, M., & Andrae, R. 2021, AJ, 161, 147, doi: [10.3847/1538-3881/abd806](https://doi.org/10.3847/1538-3881/abd806)
- Gordon, K. D., Fouesneau, M., Arab, H., et al. 2016, The Astrophysical Journal, 826, 104, doi: [10.3847/0004-637X/826/2/104](https://doi.org/10.3847/0004-637X/826/2/104)
- Green, G. M., Schlafly, E., Zucker, C., Speagle, J. S., & Finkbeiner, D. 2019, The Astrophysical Journal, 887, 93, doi: [10.3847/1538-4357/ab5362](https://doi.org/10.3847/1538-4357/ab5362)
- Green, G. M., Schlafly, E. F., Finkbeiner, D. P., et al. 2014, ApJ, 783, 114, doi: [10.1088/0004-637X/783/2/114](https://doi.org/10.1088/0004-637X/783/2/114)
- . 2015, ApJ, 810, 25, doi: [10.1088/0004-637X/810/1/25](https://doi.org/10.1088/0004-637X/810/1/25)
- Jurić, M., Ivezić, Ž., Brooks, A., et al. 2008, The Astrophysical Journal, 673, 864, doi: [10.1086/523619](https://doi.org/10.1086/523619)
- Lallement, R., Vergely, J.-L., Valette, B., et al. 2014, A&A, 561, A91, doi: [10.1051/0004-6361/201322032](https://doi.org/10.1051/0004-6361/201322032)
- Queiroz, A. B. A., Anders, F., Santiago, B. X., et al. 2018, Monthly Notices of the Royal Astronomical Society, 476, 2556, doi: [10.1093/mnras/sty330](https://doi.org/10.1093/mnras/sty330)

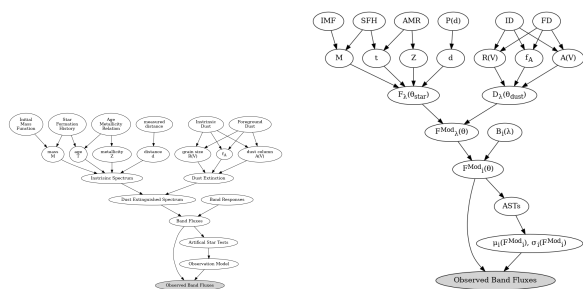


**Figure 4.** BEAST.